ACS Catalysis

RESEARCH ARTICLE

pubs.acs.org/acscatalysis

Kinetics Analysis of Palladium/Gold Nanoparticles as Colloidal Hydrodechlorination Catalysts

Yu-Lun Fang,[†] Kimberly N. Heck,[†] Pedro J. J. Alvarez,[‡,§] and Michael S. Wong[†,§,⊥,*]

[†]Department of Chemical and Biomolecular Engineering, [‡]Department of Civil and Environmental Engineering, [§]Center for Biological and Environmental Nanotechnology, and [⊥]Department of Chemistry, Rice University, 6100 South Main Street, Houston, Texas 77005, United States

Supporting Information

ABSTRACT: The aqueous-phase hydrodechlorination (HDC) of trichloroethene (TCE) is an important chemical reaction for water pollution control, for which unsupported palladium-on-gold and palladium nanoparticles (Pd/Au and Pd NPs) definitively show the beneficial effects of gold on palladium catalysis. The observed batch reactor kinetics can be erroneously oversimplified when concentration and mass transfer effects are neglected. A comprehensive treatment of NP catalysis is presented here using Pd-based NPs as the catalytic colloid and TCE HDC as the model reaction. Mass transfer effects were quantified for three specific compositions (Pd/Au NPs with 30% and 60% Pd surface coverages, and pure Pd NPs) by analyzing the observed reaction rates as functions of stirring rate and initial catalyst charge. The largest effect on observed reaction rates came from gas−liquid mass transfer. The TCE HDC reaction was modeled as a Langmuir−Hinshelwood mechanism involving competitive chemisorption of dihydrogen and TCE for all three NP compositions. Differences in adsorption affinities of the reactant molecules for the Pd/Au and Pd surfaces are suggested as responsible for the observed difference in TCE reaction order at high TCE concentrations; that is, first-order for Pd/Au NPs and non-first-order for Pd NPs.

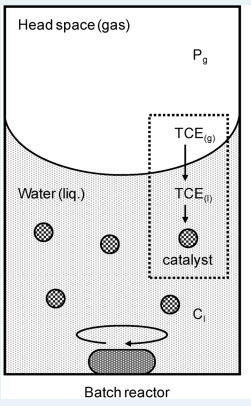

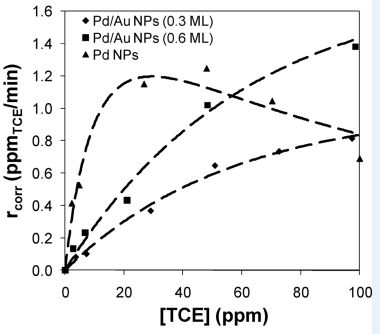

KEYWORDS: nanoparticle catalysis, palladium, gold, trichloroethene, hydrodechlorination, kinetics, mass transfer, Langmuir−Hinshelwood

1. INTRODUCTION

As an emerging field of interest during the past decade, nanoparticle (NP) catalysis encompasses chemical reactions catalyzed by NPs that are freely suspended in the liquid reaction medium or are supported on certain solids.[1−3] Examples of catalytic NP compositions include photocatalytic semiconductor metal oxides, such as TiO_2;[1,4,5] metal chalcogenides, such as CdSe ("quantum dots"[6−9]); and transition metals, such as Pd, Pt, and Rh.[1−3,6,10] As one of the extensively studied composition types, catalytic transition metal NPs have been investigated for both supported forms (including fuel cell reactions,[11−14] and hydrogenation[15−17]) and suspended colloidal forms (including reduction,[18−20] oxidation,[21−25] hydrogenation,[25−30] electron transfer reactions,[31−33] and carbon coupling reactions[34−39]). So far, the colloidal form of catalytic NPs has been studied far less than the supported form, with the latter comprising the class of supported metal catalysts.

Colloidal transition metal NPs have uniform particle sizes typically in the 1−10 nm range, well-controlled composition, well-defined shape, kinetic colloidal stability, and reproducibility in synthesis.[10,40,41] Catalysis by such NPs, referred to hereafter as colloidal NP catalysis or colloidal catalysis, has similarities to both heterogeneous and homogeneous forms.[2] From the homogeneous point-of-view, these NPs can be dispersed and handled in solvents and characterized as molecular compounds by spectroscopic techniques;[3,18−20,31−33,42−44] from the heterogeneous point-of-view, these NPs behave as metal solids with a defined particle surface.[3,11,45] As an added complication, catalysis can occur in solution due to metal leachate generated in situ, as has been established for Pd NPs in carbon coupling reactions.[36−38]

Colloidal NPs can be considered a model material for the study of supported metal catalysis in which support effects are eliminated; for example, mass transfer limitations and metal−support interactions.[6] NPs have no internal porosity, and the active sites are located exclusively at the particle surface, so intraparticle diffusion is a nonissue. Very high stirring rates are used in the batch reactions, although the assumption of negligible external

Received: October 26, 2010
Revised: December 19, 2010

diffusion is not usually verified.[21−23,26−30,46,47] The effect of stirring rate on measured reaction rates is the common method, but a more rigorous approach to analyzing the effects of mass transfer on colloidal NP catalysis is needed.

We develop such an approach in this work using palladium-on-gold (Pd/Au) NPs as the colloidal catalytic material. Pd/Au NPs is highly active for the room-temperature aqueous-phase hydrodechlorination (HDC) of trichloroethene (TCE), perchloroethene, and other chlorinated compounds dissolved in water.[48−50] Pd is a well-studied catalyst for HDC reactions,[51−53] especially for TCE.[54−63] TCE is of particular interest as one of the most common hazardous organic contaminants found in groundwater.[64−69] We showed that Pd/Au NPs were significantly more active than monometallic Pd catalysts, exhibiting maximum activity at submonolayer Pd coverages that was 2 orders of magnitude greater than Pd black on a Pd atom basis. Gold increased Pd catalytic activity through a likely combination of mixed site and electronic effects[50,70−72] and further led to deactivation resistance to chloride and sulfide species, a common problem for Pd-based catalysis.[73] Gold appeared to cause Pd to be more oxidation resistant compared with monometallic Pd.[74] Lab-scale flow reactor testing of immobilized Pd/Au NPs indicated a 20-fold decrease in materials cost compared with commercially available Pd/Al_2O_3.[48]

In this paper, we present an experimental protocol for studying simultaneously the surface reaction and external mass transfer rates of Pd/Au NPs and Pd NPs for TCE HDC, which improves upon our earlier effort.[50] The effects of stirring rate and catalyst charge amount in a batch reactor were analyzed to determine the relative contributions of the possible mass-transfer resistances to surface reaction. A proposed Langmuir−Hinshelwood reaction pathway was found to be consistent with the rate data for Pd/Au NPs and Pd NPs, corrected for mass transfer resistances. The kinetic analysis presented here is general and adaptable to liquid-phase reactions catalyzed by colloidal NPs.

2. EXPERIMENTAL SECTION

2.1. Catalyst Preparation. *2.1.1. Monometallic NPs.* Monometallic Au NPs and Pd NPs were synthesized in the way similar to our previous work.[50] For Au NPs, a gold salt solution was prepared by diluting 1 mL $HAuCl_4$ solution (0.236 M; $AuCl_3$ 99.99%, Sigma-Aldrich; $AuCl_3$ was dissolved in water at room temperature) in 80 mL Nanopure water (>18.0 MΩ-cm, Barnstead NANOpure Diamond). A second solution was prepared by dissolving 0.04 g of trisodium citrate (>99.5%, Fisher), 0.05 g of tannic acid (>99.5%, Sigma-Aldrich), and 0.018 g of potassium carbonate (>99.5%, Sigma-Aldrich) in 20 mL of Nanopure water. Both solutions were heated to 60 °C and kept at 60 °C for at least 5 min before mixing together. The overall fluid was kept stirring vigorously and was heated to boil for 20 min before being removed from the heat source. As observed, the color of the heated overall fluid changed with time, from light yellow to reddish, brown, and finally dark brown. Au NPs in the final fluid were of 4-nm size in diameter according to transmission electron microscopy analysis reported previously.[50,74] Elemental analysis, conducted on randomly selected, centrifuged NP samples using a PerkinElmer inductively coupled plasma optical emission spectrometer (ICP-OES) Optima 4300 DV, indicated >95% of Au salt precursor was in the NP form. We calculated the concentration of the final Au NP suspension to be 1.07×10^{14} NP/mL, based on a 100% reduction of Au salts into NPs.

The procedure for Pd NPs was almost the same as for Au NPs, except that a palladium salt solution was substituted for the gold salt solution. The palladium salt solution was prepared by diluting 12 mL H_2PdCl_4 solution (0.002 40 M), which was prepared by dissolving $PdCl_2$ (99.99%, Sigma-Aldrich) in 0.005 M $HCl_{(aq)}$ at room temperature with moderate stirring, in 68 mL Nanopure water. The overall color of the heated fluid also changed with time, from light yellow to brown. Pd NPs in the final fluid were of 4-nm size in diameter according to transmission electron microscopy analysis reported previously.[74] ICP results generally indicated >95% of the Pd salt precursor was in the NP form. We thus assumed 100% conversion of Pd salts and calculated the concentration of the final Pd NP suspension to be 1.22×10^{14} NP/mL.

2.1.2. Bimetallic Pd/Au NPs. Pd/Au NPs were also synthesized as previously reported, with the NPs modeled as gold "magic clusters" with seven complete shells of gold atoms and a Pd shell of different coverages.[50] In the preparation of Pd/Au NPs with a 30% Pd surface coverage (= 0.3 monolayer = 0.3 ML), 28.5 μL H_2PdCl_4 solution (0.002 40 M) was added to 2 mL Au NP suspension (1.07×10^{14} NP/mL) and mixed. The fluid was then bubbled with hydrogen gas (99.99%, Matheson) for 2 min and left at room temperature (22 ± 2 °C) overnight. In the preparation of Pd/Au NPs with a 60% Pd surface coverage (= 0.6 ML), 57.0 μL H_2PdCl_4 solution (0.002 40 M) was used instead. ICP results indicated >95% of Pd salt precursor was reduced and incorporated into the Pd/Au NPs. For calculation purposes, we assumed 100% conversion of Pd precursor.

2.2. Mass Transfer Catalytic Experiments. In the batch reactor studies of TCE HDC, Nanopure water and a magnetic stir bar were sealed in a screw-cap bottle (250 mL, Alltech) with PTFE-sealed threads and a PTFE-silicone septum. The initial water volume was controlled so that the final liquid reaction volume was 173 mL after addition of the colloidal sol. Hydrogen gas was bubbled into the bottle for 15 min to displace dissolved oxygen and to fill the headspace with a hydrogen atmosphere (1 atm). All the reactions were performed at room temperature.

2.2.1. Pd/Au NP Testing. After hydrogen bubbling, 3 μL of TCE (99.5%, Sigma-Aldrich) and 0.2 of μL pentane (99.7%, Burdick and Jackson) as the internal standard were injected into the sealed bottle. The overall solution was stirred for at least 3 h to reach equilibrium, then at time $t = 0$, a specific volume of Pd/Au NP (0.3 ML) suspension (0.30, 0.60, 0.90 mL; 1.07×10^{14} NP/mL) was injected into the reaction bottle at a set stirring rate (300, 600, 900 rpm). The reaction was monitored through headspace gas chromatography (GC) using an Agilent Technologies 6890N GC with a flame ionization detector (FID) and a packed column (length 1.83 m × o.d. 1/8 in. × i.d. 2.1 mm) containing 60/80 Carbopack B/1% SP-1000 (Supelco 12487, Sigma-Aldrich). The initial TCE concentration was 21.8 ppm in liquid and 3.49 ppm in gas, within the detectable FID range. TCE HDC reaction rates were determined by the initial slope of TCE concentration−time profiles within the first 5 min. Pd/Au NPs (0.6 ML) were tested in the same way but with half the NP suspension volumes (0.15, 0.30, 0.45 mL) so that the charged Pd amount was kept the same.

2.2.2. Pd NP Testing. Tests for Pd NPs were conducted slightly differently. After hydrogen bubbling, 0.3 μL of TCE and 4 μL of methylene chloride (99.9%, Fisher) as the internal standard were injected into the sealed bottle. The overall solution

Scheme 1. Mass Transfer Pathway of TCE in the Aqueous-Phase TCE HDC Reaction Catalyzed by Suspended Particles in a Batch Reactor

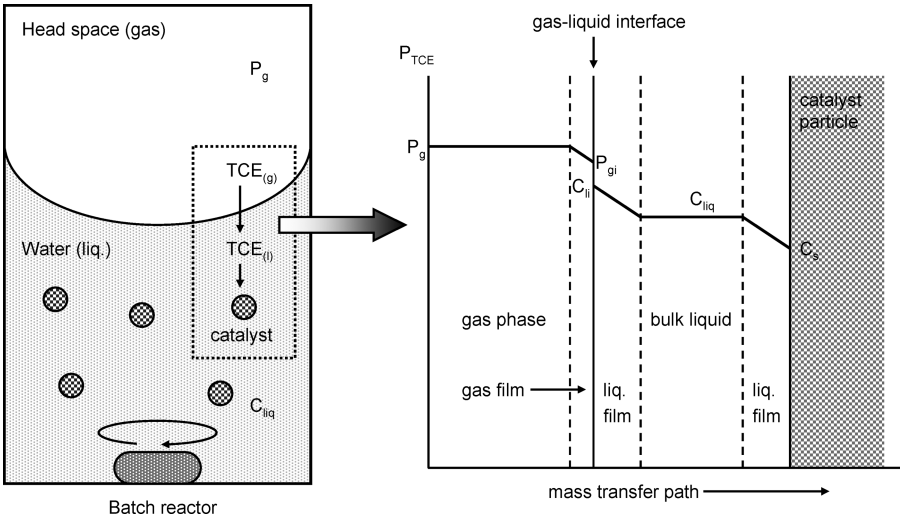

was stirred for at least 3 h to reach equilibrium, then at time $t = 0$, a specific volume of Pd NP suspension (0.28, 0.56, 1.12 mL) was injected into the bottle at a set stirring rate (300, 600, 900 rpm). The reaction was monitored through headspace GC using an Agilent Technologies 6890N GC with a microelectron capture detector (μ-ECD) and a capillary column (length 30 m × o.d. 320 μm × i.d. 0.25 μm) containing 5% phenyl methyl siloxane (HP-5, Agilent Technologies). The initial TCE concentration was 2.18 ppm in liquid and 0.349 ppm in gas, within the detectable ECD range but below the detection limit for FID. Methylene chloride was chosen as the internal standard because ECD is very sensitive to chlorine atoms. This molecule had no effect on the TCE HDC reaction[59] and did not undergo reactions (no concentration change) according to control experiments with 40 μL methylene chloride under the same conditions. TCE HDC reaction rates were determined by the initial slope of TCE concentration−time profiles within the first 5 min.

2.3. Reaction Mechanism Experiments. For this study, the TCE HDC reaction was carried out at different initial TCE concentrations, using specified amounts of TCE and an internal standard. The internal standard was either methylene chloride (4 μL) (if the initial TCE concentration in liquid $[TCE]_0$ was <20 ppm) or pentane (0.2 μL) (if $[TCE]_0 > 20$ ppm). The overall solution was stirred for at least 3 h to reach equilibrium, then at time $t = 0$, a volume of Pd/Au NP (0.3 ML) suspension (0.4 mL) was injected into the bottle, which was kept at a stirring rate of 600 rpm. The reaction was monitored using the ECD for headspace samples containing methylene chloride, or FID for headspace samples containing pentane. TCE HDC reaction rates were determined by the initial slope of TCE concentration−time profiles within the first 5 min and corrected for mass-transfer effects. For the testing of Pd/Au NPs (0.6 ML) and Pd NPs, volumes of 0.2 and 0.8 mL were used, respectively.

3. RESULTS AND DISCUSSION

3.1. Mass Transfer Analysis of NP Catalysts. *3.1.1. General Theory for Spherical Nonporous Catalytic Particles.* The NP-catalyzed TCE HDC can be considered to occur in a three-phase gas/liquid/solid reactor.[75] Scheme 1 shows the TCE transport from the headspace through liquid phase and to the catalyst particle surface.

Because surface reaction cannot be faster than TCE mass transfer, the rate of surface reaction equals to the rate of mass transfer through each of the films (rate unit = [TCE amount/time]); therefore,

$$-\frac{d[TCE]}{dt} = r_{obs} = r_{diff,g} = r_{diff,gl} = r_{diff,ls} = r_{surf\ rxn} \quad (1)$$

where

$$r_{diff,g} = k_g a_{gl}(P_g - P_{gi})/H_{TCE} \quad (2)$$

$$r_{diff,gl} = k_{gl} a_{gl}(C_{li} - C_{liq}) = k_{gl} a_{gl}(P_{li} - P_{liq})/H_{TCE} \quad (3)$$

$$r_{diff,ls} = k_{ls} a_s(C_{liq} - C_s) = k_{ls} a_s(P_{liq} - P_s)/H_{TCE} \quad (4)$$

With the assumption that the surface reaction can be described as a first-order reaction in TCE and zero-order in hydrogen (with hydrogen in excess), the rate equation (eq 1) becomes

$$r_{surf\ rxn} = k a_s C_s = k a_s P_s/H_{TCE} \quad (5)$$

In eq 5, C_s is TCE concentration at catalyst surface, and P_s is partial pressure of TCE at catalyst surface, calculated from Henry's law and C_s. Since $r_{diff,ls} = r_{surf\ rxn}$, then $k_{ls} a_s(P_{liq} - P_s) = k a_s P_s$, and P_s can be solved as

$$P_s = \frac{k_{ls} P_{liq}}{k + k_{ls}} \quad (6)$$

Substituting P_s from eq 6 into eq 4 gives

$$r_{diff,ls} = \frac{k k_{ls} a_s P_{liq}}{(k + k_{ls}) H_{TCE}} \quad (7)$$

Similarly, P_{liq} and P_{li} can be solved from eqs 2−4 and can be substituted into eq 2 to obtain

$$r_{obs} = \frac{P_g}{\left(\frac{1}{k_g a_{gl}} + \frac{1}{k_{gl} a_{gl}} + \frac{1}{k_{ls} a_s} + \frac{1}{k a_s}\right) H_{TCE}} \quad (8)$$

dx.doi.org/10.1021/cs100067k |ACS Catal. 2011, 1, 128–138

According to the literature,[76] the gas film resistance of TCE is negligible compared with liquid film; therefore, eq 8 can be simplified to

$$r_{obs} = \frac{P_g}{\left(\frac{1}{k_{gl}a_{gl}} + \frac{1}{k_{ls}a_s} + \frac{1}{ka_s}\right)H_{TCE}} \quad (9)$$

From the definition of Henry's law constant, $H = P_g/C_{liq}$, eq 9 can be rewritten as

$$r_{obs} = \frac{C_{liq}}{\frac{1}{k_{gl}a_{gl}} + \frac{1}{k_{ls}a_s} + \frac{1}{ka_s}} \quad (10)$$

Here, $1/k_{gl}a_{gl}$ and $1/k_{ls}a_s$ represent the resistances of diffusion through the liquid films at the gas−liquid interface and through the boundary layer at the liquid−particle surface, and $1/ka_s$ is the surface reaction resistance. By rearranging eq 10, one gets

$$\frac{C_{liq}}{r_{obs}} = \frac{1}{k_{gl}a_{gl}} + \frac{1}{k_{ls}a_s} + \frac{1}{ka_s} = \frac{C_1'}{a_{gl}} + \frac{C_2'}{a_s} \quad (11)$$

which simplifies to

$$\frac{1}{r_{obs}} = C_1 + \frac{C_2}{w_s} \quad (12)$$

where

$$w_s = a_s\left(\frac{d_p}{6}\right)\left(\frac{\rho_p}{\rho_{liq}}\right) \quad (13)$$

$$C_1 = \left(\frac{1}{k_{gl}a_{gl}}\right)\left(\frac{1}{C_{liq}}\right) \quad (14)$$

$$C_2 = \left(\frac{1}{k} + \frac{1}{k_{ls}}\right)\left(\frac{1}{C_{liq}}\right)\left(\frac{d_p}{6}\right)\left(\frac{\rho_p}{\rho_{liq}}\right) \quad (15)$$

Equation 12 indicates that the observed reaction rate (r_{obs}) will vary with catalyst loading (w_s), which determines the liquid−catalyst surface area; it also indicates how mixing within the batch reactor affects the observed reaction rate. A stirring rate that is high enough for gas−liquid mass transfer to be negligible would give $C_1 \sim 0$, meaning $k_{gl}a_{gl}$ is very large. A low stirring rate would decrease the gas−liquid interfacial area, a_{gl}, thereby giving a nonzero C_1 or intercept in a $(1/r_{obs})$-vs-$(1/w_s)$ plot. Thus, in this manner, the effect of stirring can be quantified. This mass transfer analysis is applicable to spherical nonporous catalytic particles of any size. This approach also applies to the general case of porous catalysts for three-phase gas/liquid/solid reactions if intraparticle porosity effects are included; for example, in industrial hydrogenation reactions.[75,77−79]

3.1.2. Applicability of Mass Transfer Model to Pd/Au and Pd NPs. So that the general analysis could be applied correctly to Pd/Au NPs (0.3 and 0.6 ML) and Pd NPs for TCE HDC, the condition of constant hydrogen concentration in the reactor needed to be satisfied. Calculations indicated that, within the 5-min time interval in which initial reaction rates were measured, the maximum consumed amounts of hydrogen were <1% of the initial amount (Table 1) and TCE conversions were <16%. Thus, the hydrogen content was in excess, and it could be approximated to be constant.

We recently found that the reaction order of TCE HDC was not necessarily always first-order in TCE and that initial TCE concentration determined the observed reaction order, depending on the Pd catalyst type.[73] Here, we were able to verify these observations by analyzing the reaction at "low" and "high" $[TCE]_0$ (Figure 1). Although the initial reaction rates were collected within the first 5 min of reaction, the concentration−time profiles of Figure 1 were reasonably well-behaved for times beyond 5 min. As expected, the reaction was first-order in TCE concentration for Pd/Au NPs at both concentrations (Figure 1a, b, d, and e).

In contrast, the reaction was first-order in TCE with Pd NPs at low $[TCE]_0$ (Figure 1c) but was not first-order at high $[TCE]_0$ (Figure 1f). The "low" $[TCE]_0$ of 2.18 ppm was close to the 1 ppm concentrations used by other research groups, in which first-order dependence was also reported.[54,80] The first-order rate constants were calculated using eq 16.

$$k_{cat} = \frac{r_{obs,0}}{[Pd][TCE]_0} = \frac{\left(\frac{-d[TCE]}{dt}\right)_0}{[Pd][TCE]_0} \quad (16)$$

3.1.3. Determination of Mass Transfer Resistances. The $(1/r_{obs})$-vs-$(1/w_s)$ plots were collected for the Pd/Au and Pd NPs (Figure 2). Each data point corresponded to a separate catalyst run at a specific catalyst charge and stirring rate, with higher catalyst amounts and faster stirring rates leading to higher observed reaction rates.

The trendlines decreased with increasing stirring rates in all cases, and the intercept C_1 was nearly zero at 900 rpm, indicating the reaction system almost reached the condition of zero gas−liquid mass transfer resistance. It was estimated that increasing from 300 to 900 rpm reduced this mass transfer resistance by ~40 times (Table 2). Calculated from the intercept C_1, the $1/k_{gl}a_{gl}$ values at 300 and 600 rpm stirring rates were similar for each NP tested (within 15% difference), indicating that gas−liquid mass transfer resistance was independent of catalyst composition (Table 2). There was greater variation in $1/k_{gl}a_{gl}$ values at 900 rpm (~30% difference), which was attributed to their smaller values, the larger effects of measurement error, and operational instability of the magnetic stirrer at 900 rpm.

The liquid−solid mass transfer coefficient k_{ls} toward a spherical particle could be estimated by the Ranz−Marshall correlation, $Sh = 2 + 0.6Re^{1/2}Sc^{1/3}$, for $2 \le Re \le 200$ and $0.6 \le Sc \le 2.7$.[81] However, the maximum Reynolds number, *Re*, is 0.0094, and the Schmidt number, *Sc*, is 362 for our catalytic colloid system at room temperature. Convection contributes negligibly to diffusive mass transfer; therefore, the Sherwood number, *Sh*, is 2. From $Sh = k_{ls}d_p/D_{TCE}$, where D_{TCE} is the diffusivity of TCE in water (1.04×10^{-5} cm^2 s^{-1} at 25 °C[82]), k_{ls} was calculated to be 0.520 m/s for 4-nm particles. Using the magic cluster model[50] and counting only the exposed surface Pd atoms, we calculated a_s as 23.9, 44.7, 121 $m^2/g_{catalyst}$ for Pd/Au NPs (0.3 ML), Pd/Au NPs (0.6 ML), and Pd NPs, respectively, giving the corresponding liquid−solid mass transfer resistance $1/k_{ls}a_s$ values listed in Table 2.

With the slope C_2 nearly the same at different stirring rates for a given NP catalyst (eq 15), the surface reaction resistance, $1/ka_s$,

dx.doi.org/10.1021/cs100067k |*ACS Catal.* 2011, 1, 128–138

Table 1. Experimental Conditions of Mass Transfer Analysis with Catalytic NPs

parameter	Pd/Au NPs (0.3 ML)	Pd/Au NPs (0.6 ML)	Pd NPs
batch reactor total volume	250 mL	250 mL	250 mL
liquid phase	173 mL	173 mL	173 mL
gas phase	77 mL	77 mL	77 mL
initial H_2 total amount	3.35×10^{-3} mol	3.35×10^{-3} mol	3.35×10^{-3} mol
liquid phase	1.50×10^{-4} mol	1.50×10^{-4} mol	1.50×10^{-4} mol
gas phase	3.20×10^{-3} mol	3.20×10^{-3} mol	3.20×10^{-3} mol
H_2 amount consumed in the first 5 min (as a percentage of initial H_2 amount charged to reactor)[a]	1.26×10^{-5} mol (0.375%)	2.10×10^{-5} mol (0.627%)	1.25×10^{-5} mol (0.373%)
initial TCE total amount	3.34×10^{-5} mol	3.34×10^{-5} mol	3.34×10^{-6} mol
liquid phase	2.87×10^{-5} mol	2.87×10^{-5} mol	2.87×10^{-6} mol
gas phase	0.47×10^{-5} mol	0.47×10^{-5} mol	0.47×10^{-6} mol
initial [TCE] in liquid phase ($[TCE]_0$)	21.8 ppm	21.8 ppm	2.18 ppm
Pd total amounts of 3 different initial catalyst charges	(1) 9.39×10^{-9} mol	(1) 9.39×10^{-9} mol	(1) 8.06×10^{-8} mol
	(2) 1.88×10^{-8} mol	(2) 1.88×10^{-8} mol	(2) 1.61×10^{-7} mol
	(3) 2.81×10^{-8} mol	(3) 2.81×10^{-8} mol	(3) 3.22×10^{-7} mol
mass fraction of catalyst with respect to total liquid (w_s, g_{Pd}/g_{liquid})	(1) 5.77×10^{-9}	(1) 5.77×10^{-9}	(1) 4.95×10^{-8}
	(2) 1.15×10^{-8}	(2) 1.15×10^{-8}	(2) 9.90×10^{-8}
	(3) 1.73×10^{-8}	(3) 1.73×10^{-8}	(3) 1.98×10^{-7}
Au total amounts of 3 different initial catalyst charges	(1) 7.53×10^{-8} mol	(1) 7.53×10^{-8} mol	(1) n/a
	(2) 1.51×10^{-7} mol	(2) 1.51×10^{-7} mol	(2) n/a
	(3) 2.26×10^{-7} mol	(3) 2.26×10^{-7} mol	(3) n/a

[a] The initial reaction rates were measured in the first 5 min. Consumed H_2 amounts were based on the reaction stoichiometry: $Cl_2C{=}CHCl + 4H_2 \rightarrow H_3C{-}CH_3 + 3HCl$.

was found to be much greater than $1/k_{ls}a_s$, indicating the mass transfer effect through the diffusion boundary layer can be neglected (Table 2). The surface reaction rate constants k ($L/m_{surf\,Pd}^2/min$), which were based on the Pd metal surface area, indicated the catalysts could be ranked in decreasing activity in the following order: Pd NPs > Pd/Au NPs (0.6 ML) > Pd/Au NPs (0.3 ML). After converting into initial turnover frequencies (TOF's) by accounting for initial TCE concentrations, we confirmed that Pd/Au NPs (0.6 ML) > Pd/Au NPs (0.3 ML) on either a per-total-Pd-atom basis or a per-surface-Pd-atom basis (Table 2), which was consistent with our previous work.[48,50]

This analysis is based on the reasonable assumption that H_2 mass transfer is faster than TCE mass transfer. Analogous to the TCE case, H_2 mass transfer can be considered to occur through the gas film and liquid film at the gas−liquid interface and the liquid film at the liquid-catalyst surface, terminating at the catalyst surface. At the gas−liquid interface, the gas film resistance is negligible compared with the liquid film resistance (10^3−10^4 difference[76,83]). Considering the liquid film resistances at both interfaces, H_2 transfer is >4 times faster than TCE due to its higher molecular diffusivity in water (4.80×10^{-5} $cm^2\,s^{-1}$ for H_2 and 1.04×10^{-5} $cm^2\,s^{-1}$ for TCE at 25 °C[82,84]). The H_2 consumed in the water phase would be replenished rapidly by the H_2 in the headspace, compared with TCE. This implies further that the water-phase hydrogen concentration can be approximated to be constant due to rapid hydrogen transport from the gas space.

To remove the effects of mass transfer (mostly due to transfer through gas−liquid interface) on observed reaction rates, we obtained reaction rate r_{corr} values by setting the mass-transfer resistances $1/k_{gl}a_{gl}$ and $1/k_{ls}a_s$ in eq 10 to zero, such that $r_{corr} = C_{liq}/(1/ka_s)$. The corrected rate constants were then calculated in the following way:

$$k_{cat,\,corr} = \frac{r_{corr}}{[Pd][TCE]_0} \tag{17}$$

It can be seen that mass transfer depressed observed rates significantly. For reactions carried out at a 600-rpm stirring rate, the measured rate constants k_{cat} for Pd/Au NPs (0.3 ML), Pd/Au NPs (0.6 ML), and Pd NPs were lower than the corrected values $k_{cat,\,corr}$ by 24%, 33%, and 51% (Table 2).

Other measured rates can be corrected for mass transfer effects without resorting to collecting additional $(1/r_{obs})$-vs-$(1/w_s)$ data, once $1/k_{gl}a_{gl}$ is known at a stirring rate and $1/k_{ls}a_s$ is neglected. It should be recognized that the gas−liquid mass transfer resistance $1/k_{gl}a_{gl}$ is not affected by catalyst composition or kinetics of the surface reaction.

TCE HDC performed with an initial liquid-phase $[TCE]_0$ = 2.18 ppm had observed rate constants k_{cat} of 2530, 4560, and 775 $L/g_{Pd}/min$ for Pd/Au NPs (0.3 ML), Pd/Au NPs (0.6 ML), and Pd NPs, at a 600-rpm stirring rate (Figure 1). Calculations gave corrected rate constants, $k_{cat,\,corr}$, of 2940, 6370, and 1170 $L/g_{Pd}/min$ for Pd/Au NPs (0.3 ML), Pd/Au NPs (0.6 ML), and Pd NPs, respectively (Table 3). The activity order was Pd/Au NPs (0.6 ML) > Pd/Au NPs (0.3 ML) > Pd NPs, consistent with previous results.[50]

3.2. Kinetics Studies for Reaction Mechanism. *3.2.1. General Rate Expression.* To gain insight into the effects of TCE concentration on reaction order as illustrated in Figure 1, we developed and tested a Langmuir−Hinshelwood model for TCE HDC after assuming the reaction proceeded through the same sequential dechlorination pathway on all catalyst compositions[48] and correcting the measured reaction rates for mass transfer effects. We also assumed that the citrate salt species were bound loosely

dx.doi.org/10.1021/cs100067k |ACS Catal. 2011, 1, 128–138

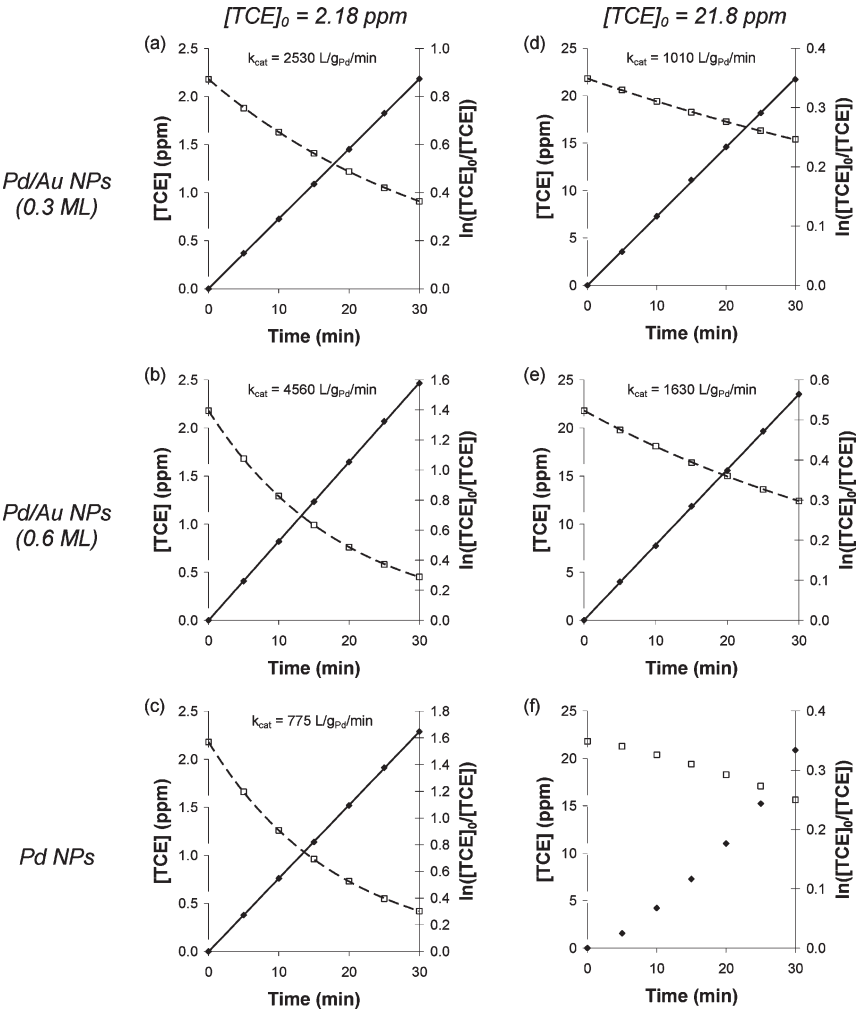

Figure 1. TCE concentration profiles in liquid phase (□) with first-order fits (– – –) and first-order linearizations (—) of TCE HDC batch reactions with different catalytic NPs and initial TCE concentrations. These reactions were carried out with a 600-rpm stirring rate.

to the NP surface through electrostatics, such that the citrate provided access to the NP surface and colloidal stability to the NP suspensions,[85,86] and that citrate did not compete for adsorption sites with TCE and H_2. Citrate and other ionic ligands are unlike other NP stabilizers, such as polymers[87,88] and dendrimers,[89,90] that are bound strongly to the NP surface to block active sites.[85]

The following general rate equation was obtained (Supporting Information):

$$\frac{-\mathrm{d[TCE]}}{\mathrm{d}t} = r_{\mathrm{corr}} = \frac{kK_{H_2}{}^{1/2}K_{\mathrm{TCE}}[\mathrm{S}]_{\mathrm{total}}{}^{2}[\mathrm{H_2}]^{1/2}[\mathrm{TCE}]}{\left(1+K_{H_2}{}^{1/2}[\mathrm{H_2}]^{1/2}+K_{\mathrm{TCE}}[\mathrm{TCE}]\right)^{2}} \quad (18)$$

If the water-phase hydrogen concentration is in excess and approximately constant due to rapid hydrogen transport from the gas space, this simplifies to

$$\frac{-\mathrm{d[TCE]}}{\mathrm{d}t} = \frac{\alpha[\mathrm{TCE}]}{(1+\beta[\mathrm{TCE}])^{2}} \quad (19)$$

where

$$\alpha = \frac{kK_{H_2}{}^{1/2}K_{\mathrm{TCE}}[\mathrm{S}]_{\mathrm{total}}{}^{2}[\mathrm{H_2}]^{1/2}}{\left(1+K_{H_2}{}^{1/2}[\mathrm{H_2}]^{1/2}\right)^{2}} \quad (20)$$

$$\beta = \frac{K_{\mathrm{TCE}}}{1+K_{H_2}{}^{1/2}[\mathrm{H_2}]^{1/2}} \quad (21)$$

If TCE concentration is very low, eq 19 can be further simplified to

$$\frac{-\mathrm{d[TCE]}}{\mathrm{d}t} = \alpha[\mathrm{TCE}] \quad (22)$$

which is consistent with the pseudo-first-order TCE HDC kinetics that are usually (but not always) observed.

3.2.2. Fitting of Experimental Data. Batch experiments at different initial TCE concentrations with catalytic NPs were carried out according to conditions listed in Table 4. The maximum consumed amounts of hydrogen were <1.1% of the total amount charged to the reactor. The reaction rates (measured at 600 rpm, corrected for mass transfer effects, and normalized by surface Pd atoms) increased with [TCE] for Pd/Au NPs (Figure 3a); however, the reaction rate profile for Pd NPs reached a maximum before decreasing at higher [TCE], an

dx.doi.org/10.1021/cs100067k |*ACS Catal.* 2011, 1, 128–138

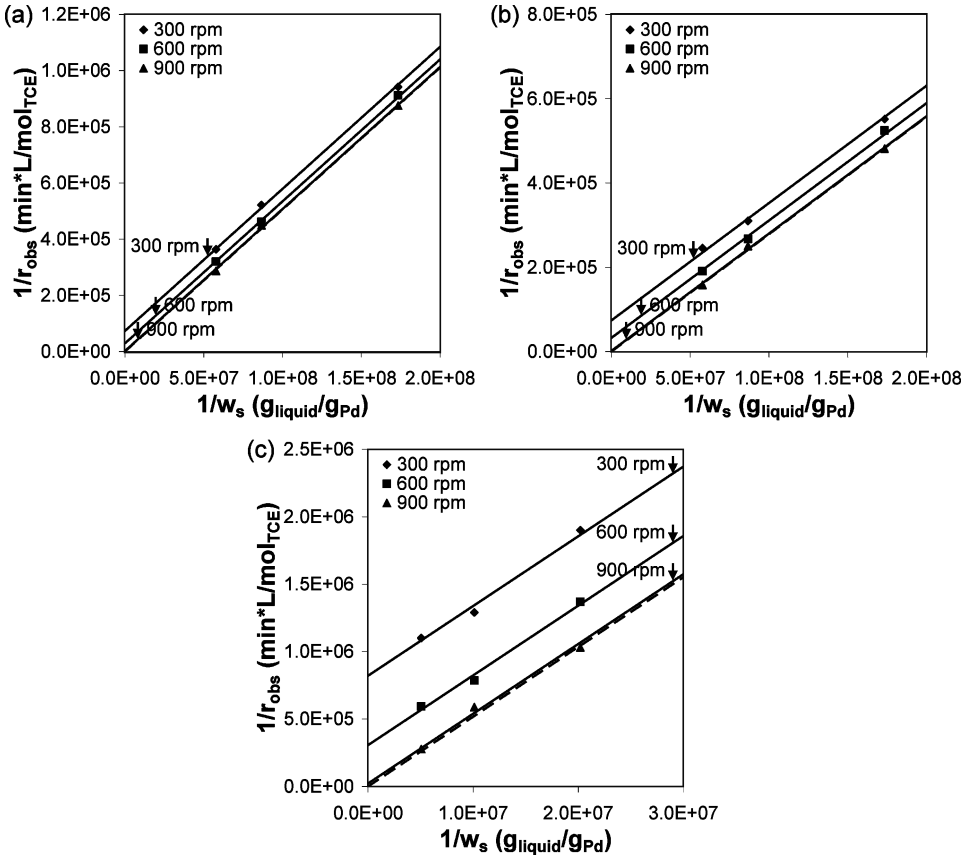

Figure 2. The relationship between $1/r_{obs}$ and $1/w_s$ for the mass transfer analysis of catalytic NPs (a) Pd/Au NPs (0.3 ML), (b) Pd/Au NPs (0.6 ML), and (c) Pd NPs. Dashed lines indicated zero gas−liquid mass transfer resistance.

Table 2. Mass Transfer Resistances and Rate Constants for TCE HDC Reactions with NPs

term	resistance type	unit	Pd/Au NPs (0.3 ML)	Pd/Au NPs (0.6 ML)	Pd NPs
$1/k_{gl}a_{gl}$ (300 rpm)	gas−liquid	min	12.2	12.3	13.6
$1/k_{gl}a_{gl}$ (600 rpm)	gas−liquid	min	4.84	5.39	5.09
$1/k_{gl}a_{gl}$ (900 rpm)	gas−liquid	min	0.300	0.252	0.377
$1/ka_s + 1/k_{ls}a_s$		min	43.6	26.1	8.66
$1/k_{ls}a_s$	liquid−solid	min	0.00478	0.00519	0.00161
$1/ka_s$	solid surface	min	43.6	26.1	8.66
k^a		$L/m_{surf\ Pd}{}^2/min$	3.58	6.21	
k^b		$L/m_{surf\ Pd}{}^2/min$			9.62
initial TOF[a]		$mol_{TCE}/mol_{Pd}/s$	0.368	0.636	
		$mol_{TCE}/mol_{surf\ Pd}/s$	0.368	0.636	
initial TOF[b]		$mol_{TCE}/mol_{Pd}/s$			0.0344
		$mol_{TCE}/mol_{surf\ Pd}/s$			0.0990
$k_{cat,\ corr}{}^a$		$L/g_{Pd}/min$	1250	2160	
		$L/g_{surf\ Pd}/min$	1250	2160	
$k_{cat,\ corr}{}^b$		$L/g_{Pd}/min$			1170
		$L/g_{surf\ Pd}/min$			3360
k_{cat} (600 rpm)[a]		$L/g_{Pd}/min$	1010	1630	
		$L/g_{surf\ Pd}/min$	1010	1630	
k_{cat} (600 rpm)[b]		$L/g_{Pd}/min$			775
		$L/g_{surf\ Pd}/min$			2230

[a] Initial liquid-phase $[TCE]_0$ = 21.8 ppm. [b] Initial liquid-phase $[TCE]_0$ = 2.18 ppm.

observation not reported before. The activity trend of Pd/Au NPs (0.6 ML) > Pd/Au NPs (0.3 ML) > Pd NPs was clear at all TCE concentrations. This trend was consistent with our previous work, which was performed at 60−70 ppm TCE.[48,50]

dx.doi.org/10.1021/cs100067k |ACS Catal. 2011, 1, 128–138

Table 3. Reaction Rates for TCE HDC Reactions with NPs at $[TCE]_0$ = 2.18 ppm

term	unit	Pd/Au NPs (0.3 ML)	Pd/Au NPs (0.6 ML)	Pd NPs
r_{obs} (600 rpm)	$mol_{TCE}/L/min$	4.84×10^{-7}	8.75×10^{-7}	1.21×10^{-6}
k_{cat} (600 rpm)	$L/g_{Pd}/min$	2530	4560	775
	$L/g_{surf\ Pd}/min$	2530	4560	2230
r_{corr}	$mol_{TCE}/L/min$	5.64×10^{-7}	1.22×10^{-6}	1.92×10^{-6}
r_{corr}	ppm_{TCE}/min	0.0741	0.160	0.252
initial TOF	$mol_{TCE}/mol_{Pd}/s$	0.0865	0.187	0.0344
	$mol_{TCE}/mol_{surf\ Pd}/s$	0.0865	0.187	0.0990
$k_{cat,\ corr}$	$L/g_{Pd}/min$	2940	6370	1170
	$L/g_{surf\ Pd}/min$	2940	6370	3360

Table 4. Experimental Conditions of Kinetic Studies with Catalytic NPs

parameter	Pd/Au NPs (0.3 ML)	Pd/Au NPs (0.6 ML)	Pd NPs
batch reactor total volume	250 mL	250 mL	250 mL
liquid phase	173 mL	173 mL	173 mL
gas phase	77 mL	77 mL	77 mL
initial H_2 total amount	3.35×10^{-3} mol	3.35×10^{-3} mol	3.35×10^{-3} mol
liquid phase	1.50×10^{-4} mol	1.50×10^{-4} mol	1.50×10^{-4} mol
gas phase	3.20×10^{-3} mol	3.20×10^{-3} mol	3.20×10^{-3} mol
max consumed H_2 amount	2.14×10^{-5} mol (0.64%)	3.64×10^{-5} mol (1.09%)	3.42×10^{-5} mol (1.02%)
(as a percentage of initial H_2 amount charged to reactor)			
initial TCE total amount (86% in liquid, 14% in gas)	10^{-8}–10^{-4} mol	10^{-8}–10^{-4} mol	10^{-8}–10^{-4} mol
initial [TCE] in liquid phase ($[TCE]_0$)	10^{-2}–10^{2} ppm	10^{-2}–10^{2} ppm	10^{-2}–10^{2} ppm
Pd total amount	1.25×10^{-8} mol	1.25×10^{-8} mol	2.30×10^{-7} mol
surface Pd amount[a]	1.25×10^{-8} mol	1.25×10^{-8} mol	8.00×10^{-8} mol
surface Pd concentration in liquid phase	7.23×10^{-8} mol/L	7.23×10^{-8} mol/L	4.62×10^{-7} mol/L
Au total amount	1.01×10^{-7} mol	5.03×10^{-8} mol	n/a

[a] Surface Pd amounts were calculated from the magic cluster model with 4-nm particles.

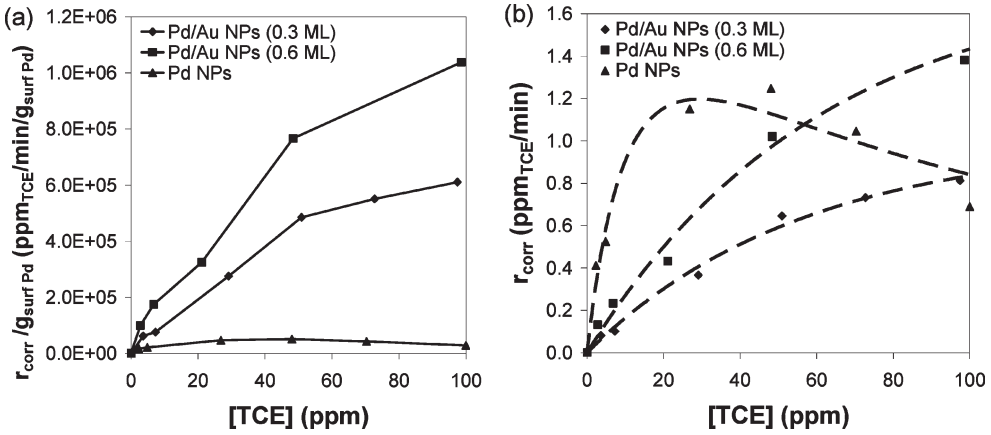

Figure 3. TCE HDC reaction rate profiles for Pd/Au NPs (0.3 ML), Pd/Au NPs (0.6 ML), and Pd NPs at different TCE concentrations: (a) normalized to surface Pd content and (b) not normalized to surface Pd content, shown with fitted curves for reaction model (dashed line). The reaction rates were measured at 600 rpm and corrected for mass transfer effects.

We performed nonlinear regression of the reaction rate data to the simplified rate expression (eq 19) and found that the Langmuir–Hinshelwood reaction model fit reasonably well (parameters shown in Table 5). Figure 3b shows the fitted curves with the corrected reaction rates. Both Pd/Au NP compositions exhibited more similar to first-order behavior, as reflected by the much smaller β values compared with the β value for Pd NPs (Table 5). This suggested that TCE had a lower adsorption affinity for the Pd/Au NP surface, that H_2 had a higher adsorption affinity, or both, according to eq 19. The latter point is consistent with reports that hydrogen binding to Pd atoms supported on a Au substrate is stronger than that for a pure Pd substrate.[91−93] This enhancement in H_2 adsorption caused by Au may be correlated to its electronic effect on Pd.[94−100] In contrast, Pd NPs exhibited a maximum in TCE HDC activity, indicating a higher TCE adsorption affinity that contributes to competitive

dx.doi.org/10.1021/cs100067k |ACS Catal. 2011, 1, 128–138

Table 5. Fitted Parameters of the Proposed Langmuir-Hinshelwood Mechanism

fitted parameter	Pd/Au NPs (0.3 ML)	Pd/Au NPs (0.6 ML)	Pd NPs
α	0.0180	0.0295	0.163
β	0.00470	0.00436	0.0340
α'	3.44×10^{12}	5.64×10^{12}	7.64×10^{11}
γ	7.33×10^{14}	1.29×10^{15}	2.25×10^{13}

Table 6. Comparison among Ratios of Parameters in the TCE HDC Reaction Mechanism

ratio	$\frac{\text{Pd/Au NPs (0.3 ML)}}{\text{(Pd/Au NPs (0.6 ML)}}$	$\frac{\text{Pd/Au NPs (0.3 ML)}}{\text{Pd NPs}}$	$\frac{\text{Pd/Au NPs (0.6 ML)}}{\text{Pd NPs}}$
$\gamma_{catalyst1}/\gamma_{catalyst2}$	0.57	33	58
$k_{catalyst1}/k_{catalyst2}$[a]	0.46	0.88	1.9

[a] $k_{catalyst1}/k_{catalyst2} = k_{cat,\ corr1}/k_{cat,\ corr2}$ from data in Table 3. Initial liquid-phase $[TCE]_0 = 2.18$ ppm.

adsorption with itself, a lower H_2 adsorption affinity compared to the Pd/Au NPs, or both.

We gained information about relative H_2 adsorption affinities by examining the fitted parameters in the following way. We defined two parameters, α' and γ:

$$\alpha' = \frac{\alpha}{[S]_{total}^{\ 2}} = \frac{k K_{H_2}^{\ 1/2} K_{TCE} [H_2]^{1/2}}{\left(1 + K_{H_2}^{\ 1/2} [H_2]^{1/2}\right)^2} \quad (23)$$

$$\gamma = \frac{\alpha'}{\beta} = \frac{k K_{H_2}^{\ 1/2} [H_2]^{1/2}}{1 + K_{H_2}^{\ 1/2} [H_2]^{1/2}} \quad (24)$$

α' is α normalized by the square of the active site concentration, therefore becoming independent of the catalyst amount. We assumed that the number of active sites equaled the number of surface Pd atoms (Table 4). γ is the ratio of α' and β, and is proportional to k, the surface reaction rate constant of the rate-limiting step (the substitution of a Cl atom in TCE with a H atom, Supporting Information). We then compared the γ and k values of the three catalysts by calculating their ratios for different pairs of catalysts (Table).

By relating these ratio values to one another using eq 25,

$$\frac{\gamma_{catalyst1}}{\gamma_{catalyst2}} = \frac{k_{catalyst1}}{k_{catalyst2}} \times \frac{\dfrac{K_{H_2,\,catalyst1}^{\ 1/2} [H_2]^{1/2}}{1 + K_{H_2,\,catalyst1}^{\ 1/2} [H_2]^{1/2}}}{\dfrac{K_{H_2,\,catalyst2}^{\ 1/2} [H_2]^{1/2}}{1 + K_{H_2,\,catalyst2}^{\ 1/2} [H_2]^{1/2}}} \quad (25)$$

we determined that the H_2 adsorption equilibrium constants for each catalyst were related as $K_{H_2,\ Pd/Au\ NPs(0.3ML)}$:$K_{H_2,\ Pd/Au\ NPs(0.6ML)}$:$K_{H_2,\ Pd\ NPs}$ = 71:49:1. The relative magnitudes indicated that H_2 had a higher adsorption affinity for Pd/Au NPs than for Pd NPs and a higher adsorption affinity for 0.3-ML Pd/Au NPs than for 0.6-ML Pd/Au NPs.

4. CONCLUSIONS

A comprehensive analysis of aqueous-phase TCE HDC catalyzed by colloidal Pd-based NPs was carried out. The gas−liquid mass transfer coefficient, the liquid−solid mass transfer coefficient, and the surface reaction for each NP catalyst were experimentally quantified, with the gas−liquid transfer rate found to be a significant contributor to the observed reaction rate. At an initial liquid-phase TCE concentration of 2.18 ppm and a 600-rpm stirring rate, observed pseudo-first-order rate constants of Pd/Au NPs (0.6 ML), Pd/Au NPs (0.3 ML), and Pd NPs were 4560, 2530, and 775 L/g_{Pd}/min, and after correction for mass transfer, they were 6370, 2940, and 1170 L/g_{Pd}/min. At a higher initial liquid-phase TCE concentration of 21.8 ppm, the rate constants were lower, and the Pd NPs lost their first-order dependence on TCE concentration. A Langmuir−Hinshelwood model with cleavage of the first C−Cl bond of TCE as the rate-limiting step was developed, which matched the mass-transfer-corrected kinetics of each of the three Pd-based NP catalysts. Analysis of the fitted parameters provided information for the first time about the adsorption affinities of the reactants for the various catalyst surfaces. Compared with Pd NPs, Pd/Au NPs had smaller equilibrium adsorption constants for TCE, which resulted in their first-order TCE concentration dependence. Pd NPs had a higher TCE equilibrium adsorption constant, which resulted in non-first-order dependence on TCE concentration at high TCE concentrations. Pd/Au NPs had higher H_2 equilibrium adsorption constants than Pd NPs. When developed and applied properly, this rigorous approach to kinetics analysis can be useful for a variety of liquid-phase reactions and catalytically active colloidal suspensions.

■ ASSOCIATED CONTENT

Supporting Information. Derivation of TCE HDC reaction rate equation. This material is available free of charge via the Internet at http://pubs.acs.org.

■ AUTHOR INFORMATION

Corresponding Author

*Phone: +1-713-348-3511. Fax: +1-713-348-5478. E-mail: mswong@rice.edu.

■ ACKNOWLEDGMENT

This work is supported by the National Science Foundation (CBEN, EEC-0647452), the Welch Foundation (C-1676),

SABIC Americas, and Rice University. We thank Prof. Mason B. Tomson (Rice University) for use of the inductively coupled plasma optical emission spectrometer (ICP-OES) and Dr. Jie Yu, Dr. Haiping Lu, and Mr. Ping Zhang (Rice University) for assistance.

SYMBOLS AND NOTATIONS

a_{gl}, a_s	Specific areas for gas−liquid interface and catalyst solid in overall batch reactor liquid volume
C_{li}, C_{liq}, C_s	Concentrations of TCE in liquid phase at gas−liquid interface, in liquid bulk, and at catalyst surface
d_p	Mean diameter of catalyst particle
D_{TCE}	Diffusivity of TCE in water
H	Henry's law constant
k	Rate constant for surface reaction
k_{cat}	Apparent rate constant obtained from uncorrected reaction rates
$k_{cat,\ corr}$	Rate constant after correction of mass transfer
k_g, k_{gl}, k_{ls}	Mass transfer coefficients for gas, gas−liquid, and liquid−solid
K	Equilibrium constant
P_g, P_{gi}	Partial pressures of TCE in gas bulk and gas film at gas−liquid interface
P_{li}, P_{liq}, P_s	Partial pressures of TCE in liquid film at gas−liquid interface, in liquid bulk, and at catalyst surface
ρ_p	Density of catalyst particle
ρ_{liq}	Density of liquid
r_{obs}	Observed reaction rate
r_{corr}	Corrected reaction rate (without mass transfer limitations)
$r_{diff,\ g}$, $r_{diff,\ gl}$, $r_{diff,\ ls}$	Rates of mass transfer through gas film, liquid film at gas−liquid interface, and liquid−solid interface
$r_{surf\ rxn}$	Rate of surface reaction
S	Active site on catalyst surface
w_s	Mass fraction of catalyst with respect to total liquid

Subscript:

0	Initial condition

REFERENCES

(1) Lewis, L. N. *Chem. Rev.* **1993**, *93*, 2693.
(2) Astruc, D.; Lu, F.; Aranzaes, J. R. *Angew. Chem., Int. Ed.* **2005**, *44*, 7852.
(3) *Nanoparticles and Catalysis*; Astruc, D., Ed.; Wiley: Weinheim, Germany, 2008.
(4) Chen, X.; Mao, S. S. *Chem. Rev.* **2007**, *107*, 2891.
(5) Yu, J.; Murthy, V. S.; Rana, R. K.; Wong, M. S. *Chem. Commun.* **2006**, 1097.
(6) Schmid, G. *Chem. Rev.* **1992**, *92*, 1709.
(7) Efros, A. L.; Rosen, M. *Annu. Rev. Mater. Sci.* **2000**, *30*, 475.
(8) Asokan, S.; Krueger, K. M.; Colvin, V. L.; Wong, M. S. *Small* **2007**, *3*, 1164.
(9) Talapin, D. V.; Mekis, I.; Gotzinger, S.; Kornowski, A.; Benson, O.; Weller, H. *J. Phys. Chem. B* **2004**, *108*, 18826.
(10) Roucoux, A.; Schulz, J.; Patin, H. *Chem. Rev.* **2002**, *102*, 3757.
(11) Bonnemann, H.; Richards, R. M. *Eur. J. Inorg. Chem.* **2001**, 2455.
(12) Haruta, M. *J. New Mater. Electrochem. Syst.* **2004**, *7*, 163.
(13) Hashmi, A. S. K.; Hutchings, G. J. *Angew. Chem., Int. Ed.* **2006**, *45*, 7896.
(14) Weiher, N.; Bus, E.; Delannoy, L.; Louis, C.; Ramaker, D. E.; Miller, J. T.; van Bokhoven, J. A. *J. Catal.* **2006**, *240*, 100.
(15) Grunes, J.; Zhu, J.; Anderson, E. A.; Somorjai, G. A. *J. Phys. Chem. B* **2002**, *106*, 11463.
(16) Bianchini, C.; Dal Santo, V.; Meli, A.; Moneti, S.; Moreno, M.; Oberhauser, W.; Psaro, R.; Sordelli, L.; Vizza, F. *J. Catal.* **2003**, *213*, 47.
(17) Boudjahem, A. G.; Monteverdi, S.; Mercy, M.; Bettahar, M. M. *J. Catal.* **2004**, *221*, 325.
(18) Jana, N. R.; Wang, Z. L.; Pal, T. *Langmuir* **2000**, *16*, 2457.
(19) Sau, T. K.; Pal, A.; Pal, T. *J. Phys. Chem. B* **2001**, *105*, 9266.
(20) Ghosh, S. K.; Mandal, M.; Kundu, S.; Nath, S.; Pal, T. *Appl. Catal., A* **2004**, *268*, 61.
(21) Comotti, M.; Della Pina, C.; Matarrese, R.; Rossi, M. *Angew. Chem., Int. Ed.* **2004**, *43*, 5812.
(22) Beltrame, P.; Comotti, M.; Della Pina, C.; Rossi, M. *Appl. Catal., A* **2006**, *297*, 1.
(23) Tsunoyama, H.; Sakurai, H.; Tsukuda, T. *Chem. Phys. Lett.* **2006**, *429*, 528.
(24) Hoover, N. N.; Auten, B. J.; Chandler, B. D. *J. Phys. Chem. B* **2006**, *110*, 8606.
(25) Crump, C. J.; Gilbertson, J. D.; Chandler, B. D. *Top. Catal.* **2008**, *49*, 233.
(26) Bronstein, L. M.; Chernyshov, D. M.; Volkov, I. O.; Ezernitskaya, M. G.; Valetsky, P. M.; Matveeva, V. G.; Sulman, E. M. *J. Catal.* **2000**, *196*, 302.
(27) Ozkar, S.; Finke, R. G. *J. Am. Chem. Soc.* **2002**, *124*, 5796.
(28) Bonnemann, H.; Braun, G. A. *Angew. Chem., Int. Ed. Engl.* **1996**, *35*, 1992.
(29) Hirai, H.; Yakura, N.; Seta, Y.; Hodoshima, S. *React. Funct. Polym.* **1998**, *37*, 121.
(30) Dash, P.; Dehm, N. A.; Scott, R. W. J. *J. Mol. Catal. A: Chem.* **2008**, *286*, 114.
(31) Narayanan, R.; El-Sayed, M. A. *J. Phys. Chem. B* **2003**, *107*, 12416.
(32) Freund, P. L.; Spiro, M. *J. Phys. Chem.* **1985**, *89*, 1074.
(33) Sharma, R. K.; Sharma, P.; Maitra, A. *J. Colloid Interface Sci.* **2003**, *265*, 134.
(34) Beletskaya, I. P.; Cheprakov, A. V. *Chem. Rev.* **2000**, *100*, 3009.
(35) Bellina, F.; Carpita, A.; Rossi, R. *Synthesis* **2004**, 2419.
(36) Phan, N. T. S.; Van Der Sluys, M.; Jones, C. W. *Adv. Synth. Catal.* **2006**, *348*, 609.
(37) de Vries, J. G. *Dalton Trans.* **2006**, 421.
(38) Astruc, D. *Inorg. Chem.* **2007**, *46*, 1884.
(39) Narayanan, R.; El-Sayed, M. A. *Top. Catal.* **2008**, *47*, 15.
(40) Aiken, J. D.; Finke, R. G. *J. Mol. Catal. A: Chem.* **1999**, *145*, 1.
(41) Widegren, J. A.; Finke, R. G. *J. Mol. Catal. A: Chem.* **2003**, *198*, 317.
(42) Narayanan, R.; El-Sayed, M. A. *Nano Lett.* **2004**, *4*, 1343.
(43) Ghosh, S. K.; Kundu, S.; Mandal, M.; Pal, T. *Langmuir* **2002**, *18*, 8756.
(44) Panigrahi, S.; Basu, S.; Praharaj, S.; Pande, S.; Jana, S.; Pal, A.; Ghosh, S. K.; Pal, T. *J. Phys. Chem. C* **2007**, *111*, 4596.
(45) Wierenga, H. A.; Soethout, L.; Gerritsen, J. W.; Vandeleemput, B. E. C.; Vankempen, H.; Schmid, G. *Adv. Mater.* **1990**, *2*, 482.
(46) Bonnemann, H.; Braun, G. A. *Chem.—Eur. J.* **1997**, *3*, 1200.
(47) Ozkar, S.; Finke, R. G. *J. Am. Chem. Soc.* **2005**, *127*, 4800.
(48) Wong, M. S.; Alvarez, P. J. J.; Fang, Y.-L.; Akçin, N.; Nutt, M. O.; Miller, J. T.; Heck, K. N. *J. Chem. Technol. Biotechnol.* **2009**, *84*, 158.
(49) Nutt, M. O.; Hughes, J. B.; Wong, M. S. *Environ. Sci. Technol.* **2005**, *39*, 1346.
(50) Nutt, M. O.; Heck, K. N.; Alvarez, P.; Wong, M. S. *Appl. Catal., B* **2006**, *69*, 115.
(51) Urbano, F. J.; Marinas, J. M. *J. Mol. Catal. A: Chem.* **2001**, *173*, 329.
(52) Alonso, F.; Beletskaya, I. P.; Yus, M. *Chem. Rev.* **2002**, *102*, 4009.
(53) Kovalchuk, V. I.; d'Itri, J. L. *Appl. Catal., A* **2004**, *271*, 13.

(54) Lowry, G. V.; Reinhard, M. *Environ. Sci. Technol.* **1999**, *33*, 1905.
(55) Lowry, G. V.; Reinhard, M. *Environ. Sci. Technol.* **2000**, *34*, 3217.
(56) Lowry, G. V.; Reinhard, M. *Environ. Sci. Technol.* **2001**, *35*, 696.
(57) Munakata, N.; Reinhard, M. *Appl. Catal., B* **2007**, *75*, 1.
(58) Schuth, C.; Kummer, N. A.; Weidenthaler, C.; Schad, H. *Appl. Catal., B* **2004**, *52*, 197.
(59) Mackenzie, K.; Frenzel, H.; Kopinke, F. D. *Appl. Catal., B* **2006**, *63*, 161.
(60) Liu, J. C.; He, F.; Durham, E.; Zhao, D. Y.; Roberts, C. B. *Langmuir* **2008**, *24*, 328.
(61) Thompson, C. D.; Rioux, R. M.; Chen, N.; Ribeiro, F. H. *J. Phys. Chem. B* **2000**, *104*, 3067.
(62) Chen, N.; Rioux, R. M.; Ribeiro, F. H. *J. Catal.* **2002**, *211*, 192.
(63) Chen, N.; Rioux, R. M.; Barbosa, L. A. M. M.; Ribeiro, F. H. *Langmuir* **2010**, *26*, 16615.
(64) Moran, M. J.; Zogorski, J. S.; Squillace, P. J. *Environ. Sci. Technol.* **2007**, *41*, 74.
(65) Russell, H. H.; Matthews, J. E.; Sewell, G. W. *EPA/540/S-92/002*, Ground Water Issue; U.S. Environmental Protection Agency: Washington, DC, 1992.
(66) *2001 Toxics Release Inventory Public Data Release Report, 260-R-03-001*; Office of Environmental Information, U.S. Environmental Protection Agency: Washington, DC, 2003.
(67) *CERCLA Priority List of Hazardous Substances*; Agency for Toxic Substances and Disease Registry, U.S. Department of Health and Human Services: Atlanta, GA, 2007.
(68) *Toxicological Profile for Trichloroethylene*; Agency for Toxic Substances and Disease Registry, U.S. Department of Health and Human Services: Atlanta, GA, 1997.
(69) *Drinking Water Standards and Health Advisories, 822-R-06-013*, 2006 ed.; Office of Water, U.S. Environmental Protection Agency: Washington, DC, 2006.
(70) Ponec, V.; Bond, G. C. *Catalysis by Metals and Alloys*; Elsevier: Amsterdam, The Netherlands, 1995.
(71) Maroun, F.; Ozanam, F.; Magnussen, O. M.; Behm, R. J. *Science* **2001**, *293*, 1811.
(72) Behm, R. J. *Z. Phys. Chem.-Int. J. Res. Phys. Chem. Chem. Phys.* **2009**, *223*, 9.
(73) Heck, K. N.; Nutt, M. O.; Alvarez, P. J. J.; Wong, M. S. *J. Catal.* **2009**, *267*, 97.
(74) Fang, Y.-L.; Miller, J. T.; Guo, N.; Heck, K. N.; Alvarez, P. J. J.; Wong, M. S. *Catal. Today* 2010, in press, doi:10.1016/j.cattod.2010.08.010.
(75) Bartholomew, C. H.; Farrauto, R. J. *Fundamentals of Industrial Catalytic Processes*; 2nd ed.; Wiley: Hoboken, NJ, 2006.
(76) Brutsaert, W.; Jirka, G. H. *Gas Transfer at Water Surfaces*; Springer: New York, NY, 1984.
(77) *Catalytic Hydrogenation;* Cerveny, L., Ed.; Elsevier: Amsterdam, The Netherlands, 1988.
(78) Levenspiel, O. *The Chemical Reactor Omnibook*; OSU Book Stores, Inc.: Corvallis, OR, 1979.
(79) Levenspiel, O. *Chemical Reaction Engineering*; Wiley: New York, NY, 1999.
(80) Kopinke, F. D.; Mackenzie, K.; Kohler, R. *Appl. Catal. B-Environ.* **2003**, *44*, 15.
(81) Tosun, İ. *Modelling in Transport Phenomena: A Conceptual Approach*; Elsevier: Oxford, UK, 2002.
(82) Schwarzenbach, R. P.; Gschwend, P. M.; Imboden, D. M. *Environmental Organic Chemistry*; Wiley: Hoboken, NJ, 1993.
(83) *Gas Transfer at Water Surfaces*; Donelan, M. A.; Drennan, W. M.; Saltzman, E. S.; Wanninkhof, R., Eds.; American Geophysical Union: Washington, DC, 2002.
(84) Mazarei, A. F.; Sandall, O. C. *AICHE J.* **1980**, *26*, 154.
(85) Daniel, M. C.; Astruc, D. *Chem. Rev.* **2004**, *104*, 293.
(86) Turkevich, J.; Stevenson, P. C.; Hillier, J. *Discuss. Faraday Soc.* **1951**, 55.
(87) Otsuka, H.; Nagasaki, Y.; Kataoka, K. *Adv. Drug Delivery Rev.* **2003**, *55*, 403.
(88) Tsunoyama, H.; Sakurai, H.; Negishi, Y.; Tsukuda, T. *J. Am. Chem. Soc.* **2005**, *127*, 9374.
(89) Chechik, V.; Crooks, R. M. *Langmuir* **1999**, *15*, 6364.
(90) Weir, M. G.; Knecht, M. R.; Frenkel, A. I.; Crooks, R. M. *Langmuir* **2010**, *26*, 1137.
(91) Baldauf, M.; Kolb, D. M. *Electrochim. Acta* **1993**, *38*, 2145.
(92) Pandelov, S.; Stimming, U. *Electrochim. Acta* **2007**, *52*, 5548.
(93) Kibler, L. A. *Electrochim. Acta* **2008**, *53*, 6824.
(94) Nascente, P. A. P.; Decastro, S. G. C.; Landers, R.; Kleiman, G. G. *Phys. Rev. B* **1991**, *43*, 4659.
(95) Koel, B. E.; Sellidj, A.; Paffett, M. T. *Phys. Rev. B* **1992**, *46*, 7846.
(96) Hammer, B.; Morikawa, Y.; Norskov, J. K. *Phys. Rev. Lett.* **1996**, *76*, 2141.
(97) Ruban, A.; Hammer, B.; Stoltze, P.; Skriver, H. L.; Norskov, J. K. *J. Mol. Catal. A: Chem.* **1997**, *115*, 421.
(98) Roudgar, A.; Gross, A. *Phys. Rev. B* **2003**, 67.
(99) Enache, D. I.; Edwards, J. K.; Landon, P.; Solsona-Espriu, B.; Carley, A. F.; Herzing, A. A.; Watanabe, M.; Kiely, C. J.; Knight, D. W.; Hutchings, G. J. *Science* **2006**, *311*, 362.
(100) Chen, J. G.; Menning, C. A.; Zellner, M. B. *Surf. Sci. Rep.* **2008**, *63*, 201.